A
Thesis
On

Effect of octupole deformation and associated orientation on fusion dynamics of $^{16}O+^{144}Ba$, ^{224}Rn, ^{224}Ra, ^{224}Th, and ^{224}U reactions

Submitted in the fulfilment of the partial requirements for the award of degree of

Master of Science
In
Physics
(2016-2018)

Submitted by
Jivea
(301604019)

Under the guidance of

Dr. Raj Kumar
(Assistant Professor)

SCHOOL OF PHYSICS AND MATERIALS SCIENCE
Thapar Institute of Engineering & Technology
PATIALA – 147004
June 2018

A grateful heart is a beginning of greatness

I dedicate this thesis to my parents *SANJEEV KUMAR* and *SWARN LATA.* I am really thankful for proiding me the best education and inspiring me so that I can accomplish my dreams.

Certificate

This is to certify that the thesis report entitled **"Effect of octupole deformation and associated orientation on fusion dynamics of $^{16}O+^{144}Ba$, ^{224}Rn, ^{224}Ra, ^{224}Th, and ^{224}U reactions"** is submitted by **Ms. Jivea** (Roll. No. 301604019) in the fulfilment of the partial requirement for the award of degree of Master of Science in Physics from School of Physics and Materials Science, Thapar Institute of Engineering & Technology, Patiala (Punjab), India. It is an exclusive record of candidate's own research under the supervision of **Dr. Raj Kumar.** This thesis in part or full has not been submitted in any other institute for award of such kind of degree.

Jivea Date

(301604019)

Dr. Raj Kumar

(Assistant Professor)

School of Physics and Materials Science

Thapar Institute of Engineering & Technology, Patiala-147004

ACKNOWLEDGMENT

I am submitting my thesis for the fulfilment of my 'M.Sc.' degree. This work would not have been accomplished without the help, support and guidance of a large number of people. I express my deep gratitude and respect to my supervisor **Dr. Raj Kumar** (Assistant Professor, School of Physics and Materials Science) for his strong motivation, trust and constant encouragement during the course of work. I thank him for his great patience, constructive criticism and for giving me the opportunity to undertake this project.

The meaning of my life and work is incomplete without paying regards to my respected family whose blessings and continuous encouragement have shown me the path to achieve my goals.

My special thanks to **Ms. Shivani Jain,** Research scholar for her moral support, patience, love and kindness to finish this work. Thanks are also due to all the research scholar of nuclear physics lab for their timely help.

Last but not the least I express my love and respect to my family and my friends for their support, motivation, trust and constant co-operation whenever I required.

And above all, I pay my regards to the Almighty for his blessings.

(Signature)

Jivea

List of figures

List of tables

Abstract

The effect of octupole deformations and orientations is studied on the interaction potential and the fusion cross-sections of ^{16}O- based reactions. In this work the octupole deformed target are considered i.e. ^{144}Ba, ^{224}Rn, ^{224}Ra, ^{224}Th, and ^{224}U. The fusion cross-sections are calculated using Wong formula. The effect of positive and negative octupole deformations is also investigated on the interaction potential. The possible change in optimum hot orientation is also studied with the inclusion of β_3-deformations

This thesis is comprised of three Chapters. The brief description of these chapter are given as follows:

Chapter 1 gives the introduction regarding the nuclear reaction and the importance of nucleus-nucleus interaction potential, with the inclusion of deformation parameters and orientations. Beside this, the fusion probability of deformed nuclei (upto octupole) has been discussed.

Chapter 2 gives the details of the methodology which is used to describe the total interaction potential with the inclusion of deformations and orientations. The penetration probability is calculated using Hill Wheeler approximation. The detail of Wong formula and it's approximation for calculating the fusion cross-sections.

Chapter 3 discusses about the calculations and results obtained because of the interaction between the spherical choice of projectile and octupole deformed target. Afterwards, fusion cross-sections are calculated using Wong formula for ^{16}O (sph.) +^{144}Ba, ^{224}Rn, ^{224}Ra, ^{224}Th, and ^{224}U nuclear systems and conclusions are shown.

Contents

Chapter 1

Introduction:

Chapter 2

Methodology:

Chapter 3

Results and discussion:

Chapter 1

Introduction

1.1 Nuclear Reaction

The existence of Universe is possible due to the involvement of four classical elements: earth, water, air and fire. With the passage of time, the study of these elements had been explored at the atomic level. Many scientists have further explored the subatomic particles, like nucleus and electrons. The discovery of nucleus and its constituents have made a drastic and far-reaching changes in the ways of thinking towards the world of very tiniest particles. The behavior of nuclear world is very much different from the macroscopic bodies which deal with the laws of gravitation. In view of this, a branch of physics, known as Nuclear Physics, has been established to examine minutely the nuclear properties, nuclear structure, nuclear interactions, shape of nuclei, etc. Nucleus consists of strongly interacting fermions – neutrons and protons collectively called as nucleons. The neutrons and protons are strongly bound together in a volume of radius about 10^{-15} m (~1fm) which gives the evidence of a strong, attractive and short range forces acting between them, by overcoming the repulsive Coulomb force between protons. Such kind of interaction is named as the strong interaction or strong force. The nucleons interact with each other in a complicated way and can be bound in many different combinations. The interaction between two nuclei is an important tool for understanding the behaviour of colliding nuclei.

To comprehend the interaction mechanism between the projectile and target nuclei, nuclear reactions provide a way to explain the phenomena like elastic and inelastic scattering, fusion, fission, deep inelastic collision (DIC), etc. These phenomena generally depend on the angular momentum, atomic masses, excitation energy, charges of nuclei, etc. The present work is mainly focused on the nuclear fusion reaction. In the fusion process, the two colliding nuclei meet head on collision with enough kinetic energy so that it can overcome the Coulomb repulsion that occurs due to the positively charged nuclei, and subsequently form a new heavier nuclei with the release of energy. Furthermore, the nuclear reactions take place at different scale of energies provided to the incident particle. In the low-energy region, the energy given to the projectile lies below 15MeV/nucleon, for intermediate, the value lies between 15 and 500MeV/nucleon, and for the case of higher-energy region, the energy goes beyond 500MeV/nucleon.

Low energy heavy ion reactions (atomic mass$\geq$4, and atomic number$\geq$2) is a subject of interest during the past few decades. The study of heavy-ion reactions in low energy regime provides an ample opportunity to examine the barrier distribution and nucleus- nucleus interaction potential. In the present work, the main intention is to deal with the low-energy heavy-ion induced reactions to observe the possibility of fusion between deformed choices of nuclei. The distribution of nucleons inside the nucleus gives the evidence of deformations. The degree of deformation is described by the deformation parameter β_λ (λ = 2, 3, 4 stand for quadrupole, octupole, and hexadecapole, respectively). The higher multipole deformations allow one to understand the nuclear dynamics in terms of nuclear radius, ion-ion interaction potential and corresponding fusion cross-sections. Since the deformation of nuclei significantly influences the interaction between two nuclei. The description of a nuclear system on the basis of deformations is explained in the literature [1-5].

Nowadays, several ideas and methods have been introduced to have a better understanding towards fusion dynamics on the basis of deformation and associated orientations of nuclear systems.

1.2 The nucleus-nucleus interaction potential

To analyze the possibility of fusion between two colliding nuclei, the study of nucleus-nucleus potential is very essential to understand. The total interaction potential (V_{tot}) is the sum of a repulsive Coulomb potential (V_C) between positively charged nuclei, a nuclear potential (V_N) due to strong attractive interaction, and the centrifugal potential (V_ℓ) due to rotation, i.e. $V_{tot}(R) = V_C(R) + V_N(R) + V_\ell(R)$, as a function of separation distance (R) between two nuclei. At nuclear level, the Coulomb and centrifugal terms, of V_{Tot} are well defined electromagnetic forces and no adjustable parameters are required to describe these potentials. On the other hand, the short-range attractive nuclear potential is not uniquely defined. In view of this, various theoretical approaches [6-16] have been given by many physicists to explain nuclear potential. An appropriate choice of $V_N(R)$ is required to study the heavy-ion reaction dynamics, since only on the basis of Coulomb potential the interaction barrier cannot be defined. In other words, the summation of nuclear and Coulomb potential gives rise to a Coulomb barrier height, V_B(MeV), which is the maximum value of energy to oppose fusion. Figure 1.1 shows the formation of the Coulomb barrier height and a deep attractive pocket due to $V_N(R)$.

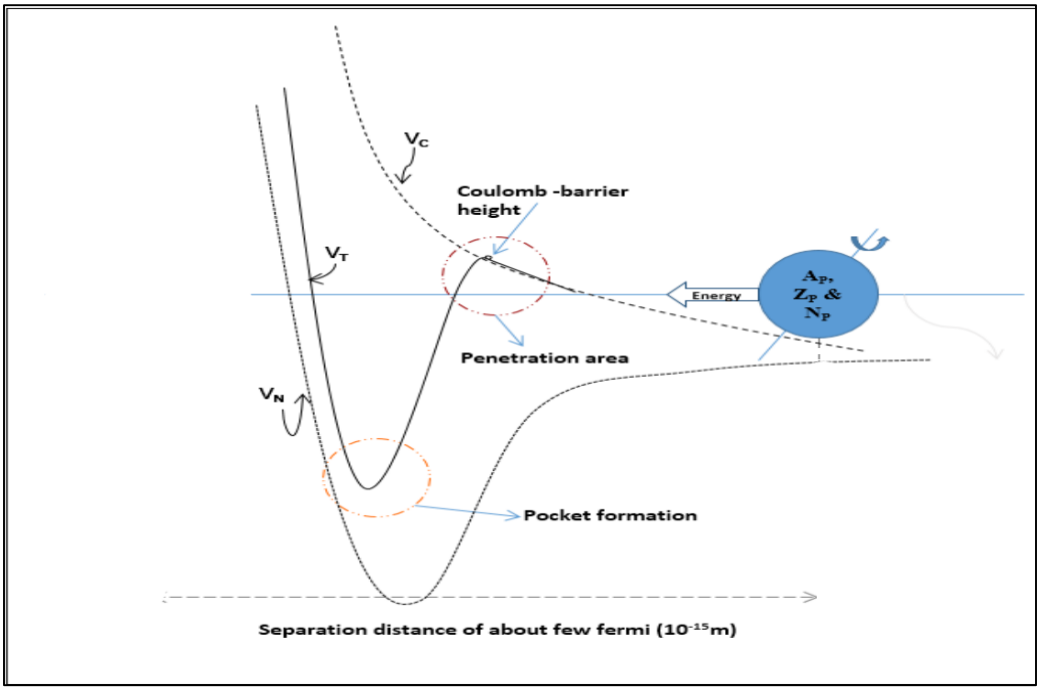

Figure 1.1 A diagram of Coulomb-barrier due to amalgamation of short-range attractive nuclear potential $V_N(R)$ and long range repulsive Coulomb potential $V_C(R)$.

There are different versions of nuclear potential which are available in the literature [6-16]. One of the most commonly used models is phenomenological model which provides a simple analytical expression to calculate the nucleus-nucleus potential, named as proximity potential. In other words, the proximity potential is defined when the two surfaces are interacting with each other in a proximity region of about 2fm (~2×10^{-15}m), where the effect of surface energy term and an additional short-range attractive force come into picture. Such proximity potentials are defined as a function of the mean curvature of the interaction surface and a universal function. The Universal function in the expression of proximity potential is only a function of separation distance between two colliding nuclei, but independent of the shapes of nuclei or geometry. The concept used to express the proximity potential plays a significant role in order to understand the nuclear fusion dynamics at low-energy regime. Various authors have given their enormous efforts to define the nuclear part of ion-ion interaction potential on the basis of the proximity theorem. At very first, Bass [6] had introduced an expression for the interaction potential and then Blocki [9] had driven a pocket formula of proximity potential .To explain the experimental results, various modifications were made in the proximity potentials via surface energy coefficient, nuclear radius, etc.

Among various available versions for nuclear proximity potential, few of them have been found reliable to explain the fusion barrier height and scattering data. In the present work, Pocket formula of Blocki *et al.* i.e. Prox77 [9] is taken into consideration to observe the nuclear fusion dynamics of heavy-ion induced low energy reactions. The interaction barrier are influenced due to the shapes of target and projectile nuclei. Hence it is an important aspect to study the effect of deformation and associated orientation in the calculation of ion-ion interaction potential.

1.3 Deformations and associated orientation:

The shape of the nucleus is one of the nuclear properties. The distribution of charges (nucleons) in the nucleus gives the evidence of deformation. The multi-pole deformed shape of a nucleus has been categorized through deformation parameter β_λ (λ = 2, 3, 4), or extreme neutron (N) to proton (Z) ratio. For λ = 2, the deformed nucleus is named as either prolate (elongated) when deformation is positive ($\beta_2>0$) or oblate (flattened shape) when β_2 is negative. The nucleus with high order deformation, like octupole ($\beta_3>0$ or <0) and hexadecapole ($\beta_4>0$ or <0), are also feasible. An apparent representation of above defined shapes of a nucleus is shown in Fig.1.2.

The shape of a deformed nucleus is symmetric around an axis, which is known as symmetric axis. Further, the interaction between the nuclei acts along a line joining the centers of two nuclei, is named as collision axis. The angle between symmetric and collision axis gives an orientation to the deformed nucleus. In view of this, the behaviour of interaction between two deformed nuclei can be analyzed with respect to the orientation. So, the inclusion of deformations and orientation within the ion-ion interaction potential would be remarkable in terms of Coulomb barrier height and corresponding effect on fusion cross-section.

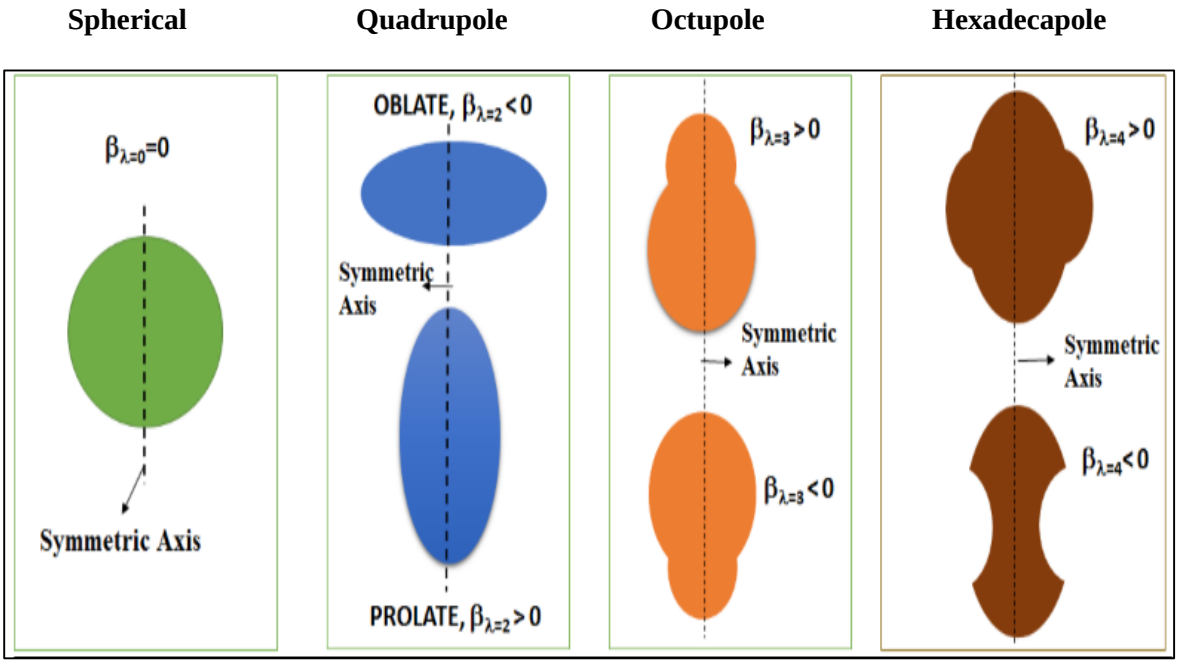

Figure 1.2 A schematic diagram of spherical, quadrupole, octupole and hexadecapole deformed nucleus.

In the present work, the main concern is to observe the effect of deformation upto octupole in the formation of a compound nuclear system. In view of this, a schematic diagram for interaction of a spherical with a prolate, and octupole shaped nucleus is represented in Fig.1.3 at different orientations, i.e. $\theta_1=\theta_2=0^o$ (no orientation), $\theta_1=0^o$, $\theta_2=90^o$, and $\theta_1=0$, $\theta_2=180^o$. From this figure, it is clearly visible that the radius of interaction between spherical and prolate nuclei changes only at 90^o, and remains same at the $\theta_2=0^o$ and 180^o. On the other hand, in the case of octupole deformation, the radius of interaction keeps changing with respect to orientation. In view of this, it would be interesting to observe influence of high order deformation and orientation on fusion barrier and fusion cross-section. The values of deformations are referred from the nuclear data table of Moller *et. al.* [17]. For the case of quadrupole nuclei, there is a symmetric or periodic variation in the radius of interaction. On the other hand, such symmetric nature disappears for the octupole deformed nucleus. As discussed earlier that, the total interaction potential is dependent on the radius of interaction between two nuclei and this radius is dependent on deformations and orientations. Later on, the variation in the Coulomb barrier height with respect to the deformation and associated orientation is detailed more clearly in Chapters- 2 and 3 of this thesis.

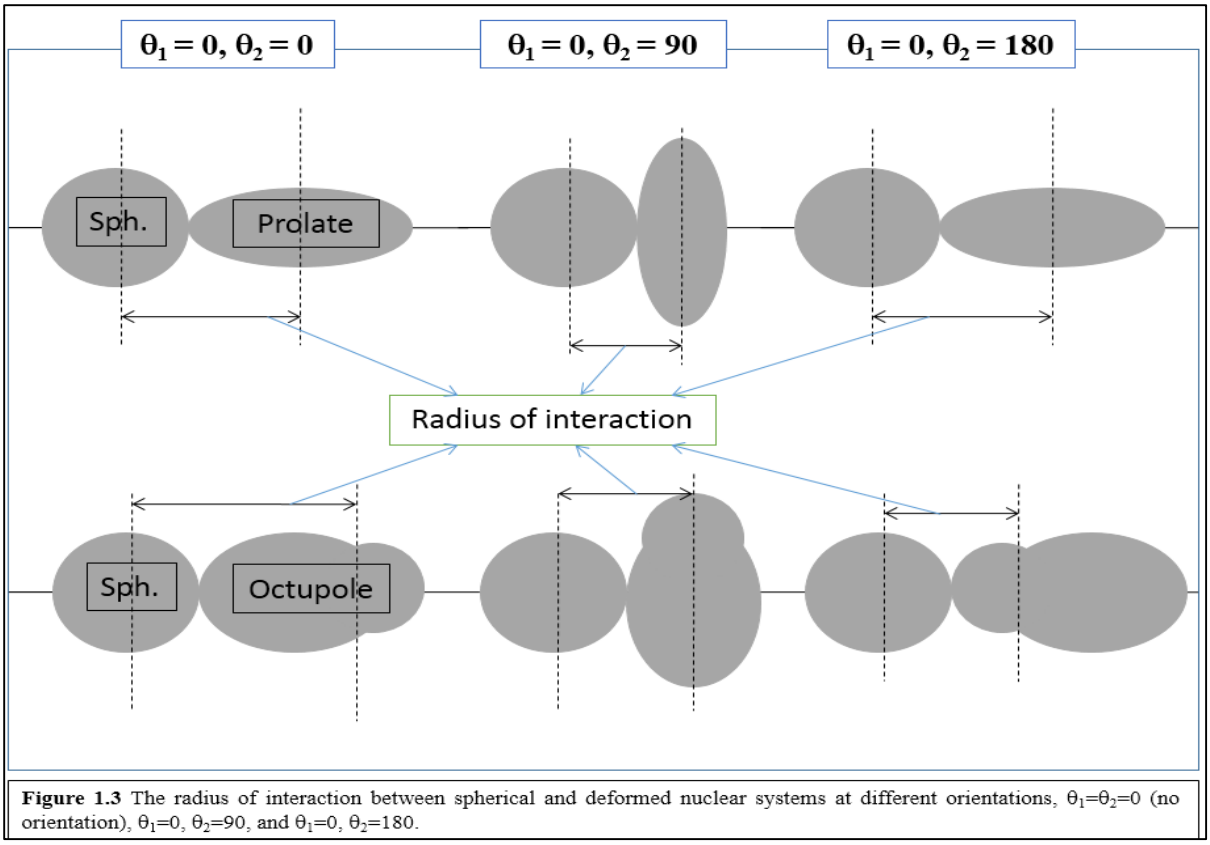

Figure 1.3 The radius of interaction between spherical and deformed nuclear systems at different orientations, $\theta_1=\theta_2=0$ (no orientation), $\theta_1=0$, $\theta_2=90$, and $\theta_1=0$, $\theta_2=180$.

1.4 Fusion cross-sections:

In the nuclear fusion mechanism, the two nuclei approach each other in the close vicinity (~2fm) to form an excited Compound Nucleus (CN). During this process, at the long range, the positively charged nuclei exerts a repulsive Coulomb force on the other one. Such force is an obstacle in the formation of a heavy particle or CN. To overcome this obstacle, the projectile requires a sufficient amount of kinetic energy so that it can enter in the proximity region, where two nuclei can have an experience of strong attractive nuclear force, as already shown in Fig.1.1. Subsequently, the penetration probability of fusion between two nuclei can be calculated. In other words, due to quantum tunneling effect, the penetration of a one dimensional barrier formed by the Coulomb, and the nuclear potentials would lead to a simple picture of fusion.

To have a systematic study of a nuclear fusion reaction, the knowledge of ion-ion interaction potential is essential, as already discussed in the above sections. In addition to this, the inclusion of deformations and associated orientations influence the barrier height of the interaction potential. Hence, this means that the fusion cross-sections and the interaction potential are largely influenced by the nuclear structure effects of target and projectile nuclei and their relative orientation. It has been already observed in the literature [17-20] that, the deformation upto quadrupole along with the orientations of colliding nuclei lowers the barrier height for 0^o and 180^o, which in turn, enhances the fusion cross-sections [21]. The lowest barrier height has the largest barrier position of an elongated configuration. On the other hand, the smallest radius of the highest barrier height give

the optimum fusion configuration. In literature [21] it has been said that the optimum orientation for quadrupole deformed nuclei is decided by signs of deformation and insensitive for the case of hexadecapole. In view of this, in the present work, the fusion barrier heights and corresponding positions will be analyzed for octupole deformed nuclei at different angles in order to find the value of optimum orientation. In the present work, the fusion cross-sections have been calculated using Wong formula [22] for octupole deformed nuclei at different orientations.

1.5 Proposed Work:

Effect of octupole deformation and associated orientation on fusion dynamics of ^{16}O+^{144}Ba, ^{224}Rn, ^{224}Ra, ^{224}Th, and ^{224}U

Nuclear fusion is an important tool for study the shape of a nucleus. For the case of octupole deformed nuclei, it has been analyzed recently in [23] that the measurement of barrier distributions clarify the presence of static octupole deformation for systems ^{16}O+^{144}Ba, and ^{224}Ra. To carry out this idea, in the present work the effect of octupole deformation along with their relative orientations has been analyzed in terms of fusion barrier heights and corresponding cross-sections. The calculations are done using Wong formula for ^{16}O+^{144}Ba, ^{224}Rn, ^{224}Ra, ^{224}Th, and ^{224}U nuclear reactions. These targets have negative β_3-deformations.

References:

[1] W. Griener, International NATO Advanced Study Institute (NASI) course on Quantum Electrodynamics of strong fields, Lahnstein 1981; M. Seiwert, N. Abul-Naga, V. Oberacker, J. A. Marahn and W. Griener, Gesellschaft fiir Schwerionen for schung (GSI) Annual Report 1981.

[2] A. J. Baltz and B. F. Bayman, Phys. Rev. C **26**, 1969 (1982).

[3] M. J. Rhoades. Brown, V. E. Oberacker, M. Seiwert and W. Griener, Z. Phys. A **310**, 287 (1983).

[4] N. Malhotra and R. K. Gupta, Phys. Rev. C **31**, 1179 (1985).

[5] A. Bohr and B. R. Mottelson, Nuclear Structure, Vol. II: Nuclear deformations , world scientific (2008)

[6] R. Bass, Phys. Lett. B **47**, 139 (1973); Nucl. Phys. A **231**, 45(1974).

[7] P. R. Christensen and A. Winther, Phys. Lett. B **65**, 19 (1976).

[8] R. Bass, Phys. Rev. Lett. **39**, 265 (1977).

[9] J. Blocki, J. Randrup, W. J. S'wia tecki, and C. F. Tsang, Ann. Phys. (NY) **105**, 427 (1977).

[10] W. Reisdorf, J. Phys. G: Nucl. Part. Phys. **20**, 1297 (1994).

[11] H. Ng^o and Ch. Ng^o, Nucl. Phys. A **348**, 140 (1980).

[12] P. M*ö*ller and J. R. Nix, Nucl. Phys. A **361**, 117 (1981).

[13] W. Reisdorf, J. Phys. G: Nucl. Part. Phys. **20**, 1297 (1994).

[14] A. Winther, Nucl. Phys. A **594**, 203 (1995).

[15] W. D. Mayers and W. J. Swiaecki, Phys. Rev. C **62**, 004610 (2000).

[16] V. Y. Denisov, Phys. Lett. B **526**, 315 (2002).

[17] P. Möller *et al*. Atomic Data and Nuclear Data Tables **109–110** 1–204 (2016).

[18] A. J. Baltz and B. F. Bayman, Phys. Rev. C **26**, 1969 (1982).

[19] M. J. Rhoades-Brown, V. E. Oberacker, M. Seiwert and W. Greiner, Z. Phys.A **310**, 287 (1983).

[20] N. Malhotra and R.K. Gupta, Phys. Rev. C **31**, 1179 (1985).

[21] R. K. Gupta *et. al.* J. Phys. G. Nucl. Part. Phys. **31**, 631-644 (2005).

[22]C. Y. Wong, Phys. Rev. Lett. **31**, 766 (1973).

[23] R. Kumar, J. A. Lay, and A. Vitturi, Phys. Rev. C **92,** 054604 (2015).

Chapter 2

Methodology

In the present work, the nuclear-nuclear interaction potential is calculated using Prox77 [14] proximity potential. Moreover, for the calculation of fusion cross-sections, Wong formula is used.

2.1 Total Interaction Potential: -

The total interaction potential (V_{Tot}) is comprised of repulsive Coulomb potential ($V_{Coul}(R)$) due to positively charged nuclei, centrifugal interaction($V_{ang.}$) and attractive nuclear potential ($V_{nucl.}$) and reads as function of separation distance between two colliding nuclei.

$$V_{Tot}(R, A_i, \beta_{\lambda i}, T, \theta_i) = V_{Coul.}(R, Z_i, \beta_{\lambda i}, T, \theta_i) + V_{ang.}(R, A_i, \beta_{\lambda i}, T, \theta_i, \ell) + V_{nucl.}(R, A_i, \beta_{\lambda i}, T, \theta_i) \quad (2.1)$$

2.1.1Coulomb potential

The Coulomb potential is termed as a mutual repulsion between two positively charged nucleus. For two deformed and oriented nuclei, the Coulomb potential reads as [1]

$$V_{coul.}(R, Z_i, \beta_{\lambda i}, \theta_i, T) = \frac{Z_{proj.}Z_{tar.}e^2}{R(T)} + \sum_{\lambda,i=1,2} \frac{3Z_{proj.}Z_{tar.}e^2}{2\lambda+1} \frac{R_i^{\lambda}(\alpha_i,T)}{R(T)^{\lambda+1}} Y_{\lambda}^{(0)}(\theta_i) \times \left[\beta_{\lambda i} + \frac{4}{7}\beta_{\lambda i}^2 Y_{\lambda}^{(0)}(\theta_i)\right] \quad (2.2)$$

Here θ_i represents the angle between the collision and symmetry axis, $Y_{\lambda}^{(0)}(\theta_i)$ is the spherical harmonics function and $\beta_{\lambda i}$ is the deformation parameter, here λ=2, 3 represents deformation for quadrupole, octupole cases, respectively. The values of these parameters are referred from the table of Moller *et al*. [2].

2.1.2Angular momentum dependent potential

The centrifugal potential is defined as the potential energy of a dynamical system, and given by

$$V_{ang.}(R, A_i, \beta_{\lambda i}, T, \ell, \theta_i) = \frac{\hbar^2 \ell(\ell+1)}{2I(T)}, \quad (2.3)$$

Here, $I(T)$ is the moment of inertia. The non-sticking limit of $I(T)$ is given as $I(T) = I_{NS} = \mu R^2$, here $\left(\mu = \frac{A_1 A_2}{A_1+A_2} m\right)$ is the reduced mass and m is nucleon mass.

2.1.3 Proximity potential for deformed and oriented nuclei

As already discussed in Chapter 1 that when two surfaces approach each other within a distance of about 2 fm, then an attractive force comes into play which brings two colliding nuclei into a closed proximity. Due to this short range attractive force, a potential arises which is named as proximity

potential. There are various versions [3-13] of proximity potentials, but in the present work, we use Prox77 [14] to observe the behavior of deformed nuclei.

Prox77 (Blocki): Blocki *et al.* [4] proposed that in close proximity the force between the two surfaces is proportional to interaction potential per unit area. This way, the expression of Blocki for spherical nuclei, on the basis of pocket formula, is given as

$$\begin{aligned} V_{\text{nucl.}}(s_0) &= f(\text{sh.}, \text{geo.})\Phi(s_0) \\ &= 4\pi\bar{R}\gamma b\Phi(s_0) \end{aligned} \tag{2.4}$$

where $\bar{R}$ is the radius curvature and has the form $\bar{R} = \frac{R_1 R_2}{R_1+R_2}$(fm), R_1 and R_2 are defined as the nuclear radius of projectile and target nuclei, respectively. The value of deformation parameter β_λ, λ=2, 3 is introduced in the following expression of nuclear radius.

Nuclear radius depends on the deformation parameter i.e.

$$R_i = R_{0i}\left[1 + \sum_{\lambda=2,3} \beta_{\lambda i} Y_{\lambda i}^{(0)}\right] = R_{0i}\left[1 + \beta_{2i} Y_{2i}^{(0)} + \beta_{3i} Y_{3i}^{(0)}\right] \tag{2.5}$$

here *i*=1, 2 stands for projectile and target respectively.

In Eq. (2.5), the half-density radius R_{0i}, is expressed as follows

$$R_{0i} = \left[1.28A_i^{1/3} - 0.76 + 0.8A_i^{-1/3}\right], \tag{2.6}$$

In Eq. (2.4), 'b'is the surface thickness parameter, γ is the surface tension and $\Phi(s_0)$ is the universal function which is considered as an independent function of the shapes of the colliding nuclei.

For deformed and oriented nuclei, the Temperature-dependent proximity potential ($V_{\text{nucl.}}(T)$) is given as [15]

$$V_N(A_i, \beta_{\lambda i}, \theta_i, T) = 4\pi\bar{R}(T)\gamma b(T)\Phi(s_0(T)), \tag{2.7}$$

where $\Phi(s_0)$, the universal function depends on the minimum separation distance s_0, and given as

$$\Phi(s_0) = \begin{cases} -\frac{1}{2}(s_0 - 2.54)^2 - 0.0852(s_0 - 2.54)^3 & s < s_0 \\ -3.437exp\left(-\frac{s_0}{0.75}\right) & s \geq s_0 \end{cases} \tag{2.8}$$

Here, s_0 is defined in units of b i.e. s_0 is s_0/b, and the T- dependent diffuseness parameter of the nuclear surface [16] is given by

$$b(T) = 0.99(1 + 0.009T^2) \tag{2.9}$$

The specific nuclear surface tension γ of Eq.(2.7) is given by

$$\gamma = \gamma_0 \left[1 - k_s \left(\frac{N-Z}{A}\right)^2\right] MeV\ fm^{-2} \tag{2.10}$$

Here, N and Z represents the total number of neutrons and protons of the compound nucleus (CN). For Proxx77, the value of γ_0 is taken to be 0.9517 $MeV\ /fm^2$ and k_s is 1.7826 $MeV\ /fm^2$.

2.2 Wong Formula

The fusion cross-sections as a function of center-of-mass energy $E_{c.m.}$(MeV), for two deformed and oriented nuclei, in terms of angular-momentum (ℓ) partial waves and is given as follows

$$\sigma(E_{c.m.}, \theta_i) = \frac{\pi}{k^2} \sum_{\ell=0}^{\ell_{\max}} (2\ell + 1) P_\ell(E_{c.m.}, \theta_i), \tag{2.11}$$

with $k = \sqrt{\frac{2\mu E_{c.m.}}{\hbar^2}}$ and μ is the reduce mass. Here, P_ℓ is the penetration probability for each ℓ which describes the penetration, using Hill-Wheeler [18] approximation of an inverted harmonic oscillator of the $V_{Tot}^{\ell}(R, E_{c.m.}$ or T, $\theta_i)$ see Eq.(2.1), in terms of the barrier height $V_B^{\ell}(E_{c.m.}, \theta_i)$ and curvature $\hbar_{\omega\ell}(E_{c.m.}, \theta_i)$ and is given as follows

$$P_\ell = \left[1 + \exp\left(\frac{2\pi\left(V_B^{\ell}(E_{c.m.}, \theta_i) - E_{c.m.}\right)}{\hbar_{\omega\ell}(E_{c.m.}, \theta_i)}\right)\right]^{-1} \tag{2.12}$$

In the above equation, the parameters $\hbar\omega_\ell(E_{c.m.}, \theta_i)$ is calculated as

$$\hbar\omega_\ell(E_{c.m.}, \theta_i) = \hbar\left[\left|d^2V^{\ell}(R)/dR^2\right| R = R_B^{\ell}/\mu\right]^{1/2} \tag{2.13}$$

and, the value of ℓ-dependent barrier position R_B^{ℓ} obtained from the following condition

$$\left|dV_T^{\ell}(R)/dR\right|_{R=R_B^{\ell}} = 0 \tag{2.14}$$

Wong calculated $\hbar\omega_\ell$ and R_B^{ℓ}using equations (2.13) and (2.14),. In other words, he had expressed $\hbar\omega_\ell$ and V_B^{ℓ} under the following mentioned approximation

(i) $\hbar\omega_\ell \approx \hbar\omega_0$,

(ii) and $V_B^{\ell} \approx V_B^0 + \frac{\hbar^2\ell(\ell+1)}{2\mu R_B^{0^2}}$, here $R_B^{\ell} \approx R_B^0$. (2.15)

In the second approximation, the value of barrier height V_B^0 which is calculated as the sum of Coulomb potential V_C (T=0) and nuclear proximity potential $V_{nucl.}$(T=0) at R=R_B^0 and becomes dependent function of deformation and orientations as given below

(2.16)

$$V_B^0\,(R = R_B^0, Zi, \beta_{\lambda i},\, E_{c.m.} \text{or T}, \theta_i) = \mathrm{V_{coul.}}(R = R_B^0, Zi, \beta_{\lambda i},\, E_{c.m.}, \theta_i) + \mathrm{V_{nucl.}}(R = R_B^0, Z_i, \beta_{\lambda i},\, E_{c.m.}, \theta_i)$$

Using the above two approximations of Eq. (2.15), and replacing the ℓ-summation in Eq. (2.12) by an integral, gives the fusion cross-section as a function of deformation (β_λ), orientations (θ) and center of mass energy ($E_{c.m.}$) as

$$\sigma(E_{c.m.}, \theta_i) = \frac{R_B^{0^2}\hbar\omega_0}{2E_{c.m.}} ln\left[1 + exp\left(\frac{2\pi}{\hbar\omega_0}(E_{c.m.} - V_B^0)\right)\right]. \tag{2.17}$$

This formula is known as Wong formula [17], for a particular orientation and deformation, the barrier characteristics are calculated from the total interaction potential, and then using Eq. (2.17), the fusion cross-section can be calculated.

References:

[1] R. K. Gupta, M. Balasubramaniam, R. Kumar, N. Singh, M. Manhas and W.Greiner, J. Phys. G: Nucl. Part. Phys. **31**, 631 (2005).

[2] P. Möller *et al*. Atomic Data and Nuclear Data Tables **109–110,** 1–204(2016).

[3] R. Bass, Phys. Lett. B **47**, 139 (1973); Nucl. Phys. A **231**, 45(1974).

[4] P. R. Christensen and A. Winther, Phys. Lett. B **65**, 19 (1976).

[5] R. Bass, Phys. Rev. Lett. **39**, 265 (1977).

[6] J. Blocki, J. Randrup, W. J. S'wia tecki, and C. F. Tsang, Ann. Phys. (NY) **105**, 427 (1977).

[7] W. Reisdorf, J. Phys. G: Nucl. Part. Phys. **20**, 1297 (1994).

[8] H. Ng^o and Ch. Ng^o, Nucl. Phys. A **348**, 140 (1980).

[9] P. M*ö*ller and J. R. Nix, Nucl. Phys. A **361**, 117 (1981).

[10] W. Reisdorf, J. Phys. G: Nucl. Part. Phys. **20**, 1297 (1994).

[11] A. Winther, Nucl. Phys. A **594**, 203 (1995).

[12] W. D. Mayers and W. J. Swiaecki, Phys. Rev. C **62**, 004610 (2000).

[13] V. Y. Denisov, Phys. Lett. B **526**, 315 (2002).

[14] J. Blocki, J. Randrup, W.J. Swiatecki, and C. F. Tsang, Ann. Phys. (N.Y.) **105**, 427 (1977).

[15] R. K. Gupta, N. Singh, and M. Manhas, Phys. Rev. C **70**, 034608 (2004).

[16] G. Royer and J. Mignen, J. Phys. G: Nucl. Part. Phys. **18**, 1781 (1992).

[17] C. Y. Wong, Phys. Rev. Lett. **31**, 766 (1973).

[18] D. L. Hill and J. A. Wheeler, Phys. Rev. **89**, 1102 (1953); T. D. Thomas, Phys. Rev. C **116**, 703 (1959).

Chapter 3

Results and discussions

Effect of octupole deformations and associated orientation on fusion dynamics of $^{16}O+^{144}Ba$, ^{224}Rn, ^{224}Ra, ^{224}Th, and ^{224}U reactions.

In the present work, the influence of octupole deformation has been analyzed in terms of the fusion barrier height and relative fusion cross-sections. The Prox77 [1] as a proximity potential has been taken into account in the calculation of the fusion barrier height, and corresponding barrier position. The, Wong formula [2] is used for calculating the fusion cross-section. In addition to this, the comprehensive analysis of quadrupole and octupole deformation is carried out to investigate their relative effects on fusion barrier heights and cross-section. The experimental data for the octupole deformed reaction partners is not presently available. Therefore, the theoretical calculations and results obtained due to a interaction between a spherical choice of projectile, ^{16}O, and the higher multi-pole deformed (octupole) targets, ^{144}Ba, ^{224}Rn, ^{224}Ra, ^{224}Th, and ^{224}U would call for an experimental verification.

The values of quadrupole and octupole deformations for the above mentioned nuclei are referred from [3] and listed in the table 3.1. The radius, as already shown in Eq. (2.9) of Chapter2, introduced in the total interaction potential is defined as a function of deformation parameter (β_λ, λ= 2, 3 for quadrupole and octupole, respectively). The radius of interaction between two nuclei is being influenced while taking the orientations from 0^o to 180^o of quadrupole and octupole deformed nuclei. In the present work, to observe the effect of the interaction of deformed nuclei along with the associated orientations, the total interaction potential as a function of separation distance or interaction radius between two colliding nuclei has been calculated for the above mentioned nuclear reactions. Henceforth, the fusion cross-sections are calculated across the Coulomb-barrier energies using the Wong formula [2] which is dependent on the barrier characteristics, i.e. barrier height V_B (MeV), barrier position R_B(fm), and barrier curvature $\hbar\omega_B$(MeV), extracted from the ion-ion interaction potential (See Eq. (2.16) of chapter 2).

Table 3.1 The value of quadrupole (β_2) and octupole (β_3) deformations for $^{16}O+^{144}Ba$, ^{224}Rn, ^{224}Ra, ^{224}Th, and ^{224}U nuclear systems.

Deformations⇨ / Reactions⇩	**Quadrupole (β_{22})**	**Octupole (β_{32})**
$^{16}O(sph.)+^{144}Ba\rightarrow^{160}Gd^*$	0.163	-0.124
$^{16}O+^{224}Rn\rightarrow^{240}Pu^*$	0.142	-0.112
$^{16}O+^{224}Ra\rightarrow^{240}Cm^*$	0.143	-0.139
$^{16}O+^{224}Th\rightarrow^{240}Cf^*$	0.144	-0.153
$^{16}O+^{224}U\rightarrow^{240}Fm^*$	0.132	-0.139

It is noted here that, we have also increased the charge number ($Z_{tar.}$) corresponding to mass number 224 of the target in order to see its effect on fusion cross-sections as well.

3.1 Observations and discussions:

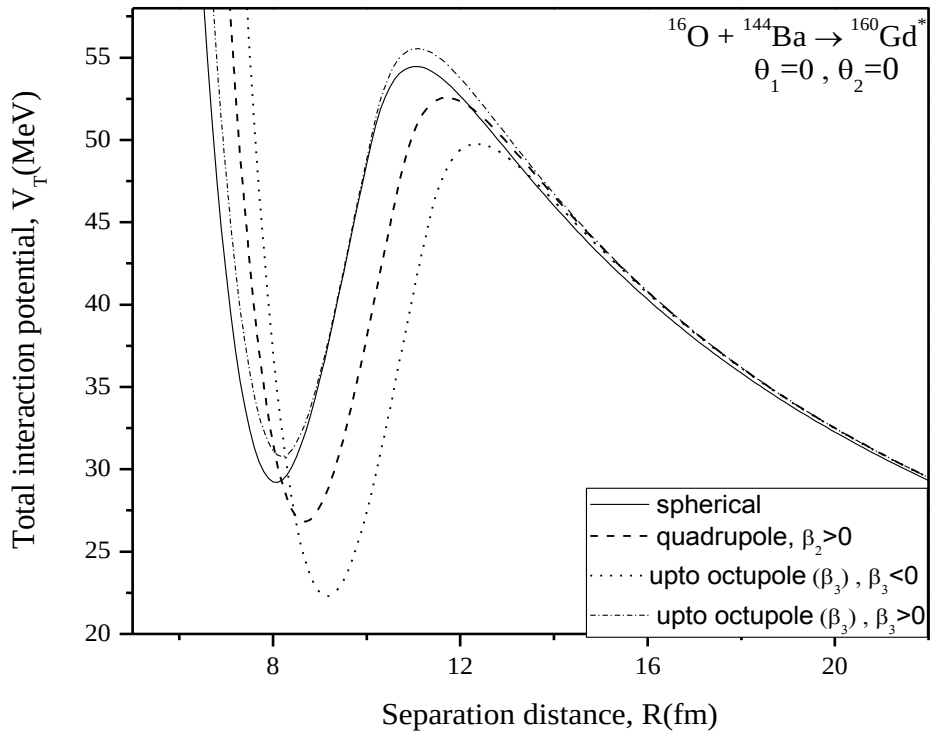

Figure 3.1 The total interaction potential (V_{Tot} (MeV)) as a function of separation distance (R(fm)) for spherical, quadrupole, and upto octupole ($\beta_3 < 0$ and $\beta_3 > 0$) deformed nuclei of $^{16}O+^{144}Ba$ reaction at T = 0 MeV.

In the present calculations, to understand the fusion dynamics of deformed nuclei upto octupole, the ion-ion interaction potential (V_{Tot} (MeV)) as a function of separation distance (R(fm)) has been analyzed firstly for $^{16}O+^{144}Ba$ reaction with the consideration of spherical, quadrupole, and upto octupole ($\beta_3 < 0$ and $\beta_3 > 0$) deformations, as shown in Fig.3.1. In this figure, it has been observed that the barrier height (V_B (MeV)) of quadrupole ($\beta_2 > 0$) followed by the octupole ($\beta_3 < 0$) case is lower than the spherical one, while there is no orientation ($\theta_1=\theta_2=0$) between the symmetric and collision axis of the colliding nuclei. In reference to spherical, V_B(MeV) of ($\beta_2 > 0$) and ($\beta_3 < 0$) shifts towards right. Additionally, by changing the sign of octupole deformations i.e. ($\beta_3 = 0.124$) for ^{144}Ba nucleus, the barrier height becomes highest and corresponding barrier position is the lowest one. In view of this, it can be said that behavior of β_3 positive and negative octupole deformed nucleus is reversible, when there is no orientation taken into account. The inclusion of deformation upto octupole ($\beta_3 < 0$), lowers the barrier height about 5MeV from the spherical case. The differences observed in the barrier heights may influence the fusion cross-section significantly.

In the present work, we have considered different nuclear reactions by keeping^{16}O as a spherical projectile with choices of octupole deformed targets, i.e. $^{16}O+^{144}Ba$, ^{224}Rn, ^{224}Ra, ^{224}Th, and ^{224}U.

Since it is known that with the inclusion of octupole deformation upto β_3 the symmetry breaks, whereas upto β_2 only, the symmetric pattern remains intact. So, it would be interesting to observe the behaviour of barrier height at $\theta=0^o$, 90^o, 180^o in order to analyze the symmetric pattern around 90^o. To carry out this idea, it is observed from Fig.3.2 that on the inclusion of orientations along with the deformation, the barrier height get significantly modified. Fig. 3.2 shows that barrier height for the five reactions considered with no orientation. The value of barrier height for spherical case is greater than quadrupole and octupole, as already noticed in the previous figure for $^{16}O+^{144}Ba$ system. It is well known that, the value of V_B for spherical remains same at all orientations as shown in all panels of Fig.3.2. In the case of quadrupole deformation, the variation in V_B is found only at 90^o is clear from Fig. 3.2. In other words, it can be said that for quadrupole the variation in barrier height is symmetric around 90^o. Further, with the inclusion of deformations upto octupole (β_2-β_3), there is asymmetric behaviour with respect to the orientations. In other words, the symmetric behaviour of barrier height V_B and corresponding barrier position R_B disappears for octupole deformed nuclei. The results obtained from this figure are similar in behavior for all the choosen reactions.

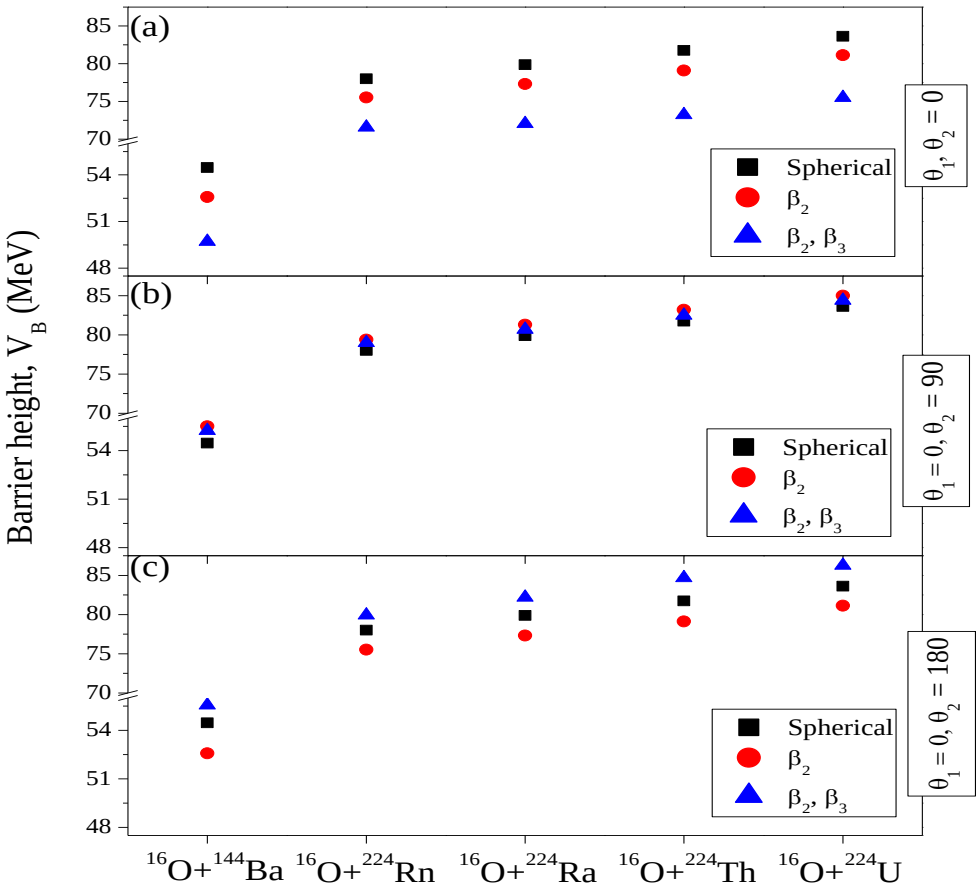

Figure 3.2 The variation in fusion barrier height (V_B (MeV)) at different orientation angles θ_2 = (a) 0^o, (b) 90^o, and (c) 180^o for $^{16}O+^{144}Ba$, ^{224}Rn, ^{224}Ra, ^{224}Th, and ^{224}U nuclear reactions.

From the above discussion, it has been analyzed that the octupole deformation and associated orientations show a certain impact on the barrier height. Further, to obtain the optimum orientations for octupole deformed choices of nuclear reactions, the Coulomb-barrier and corresponding barrier position has been calculated with respect to orientations.

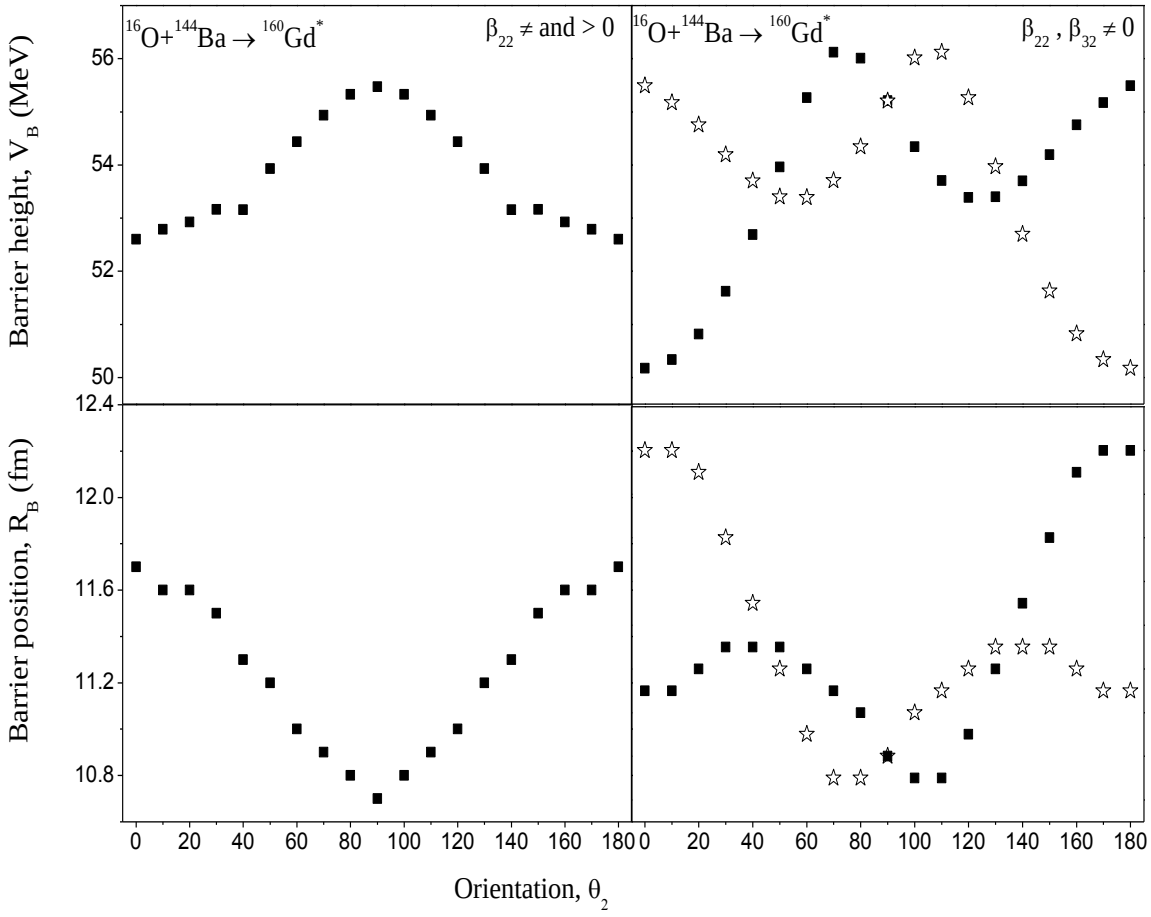

Figure 3.3 The variation in fusion barrier height (V_B (MeV)) and corresponding barrier position with respect to orientation for quadrupole and octupole deformed choices of $^{16}O+^{144}Ba$ reaction at T = 0 MeV.

From Fig.3.3, it has been observed for the case of quadrupole that, at angles 0^o and 180^o, the radius of interaction is highest, whereas it is lowest at 90^o as clearly seen through pictorial diagram represented in the same figure. Subsequently, the barrier height is found lowest for $\theta_2 = 0^o$ and 180^o, but highest at other 90^o angles. In the conclusion, it can be said that for quadrupole deformed nucleus that, the highest barrier height and lowest barrier position or radius of interaction at $\theta_2 = 90^o$ gives an hot optimum configuration. On the other hand, for octupole ($\beta_3 < 0$), the optimum orientation is found nearby 90^o. For the case of deformation upto octupole, there is no such kind of symmetric behavior in the orientation range of $\theta_2 = 0^o$ to 180^o.

Further, the fusion cross-sections have been calculated within the framework of Wong formula for spherical, quadrupole, and octupole choices of $^{16}O+^{144}Ba$, ^{224}Rn, ^{224}Ra, ^{224}Th and ^{224}U nuclear reactions.

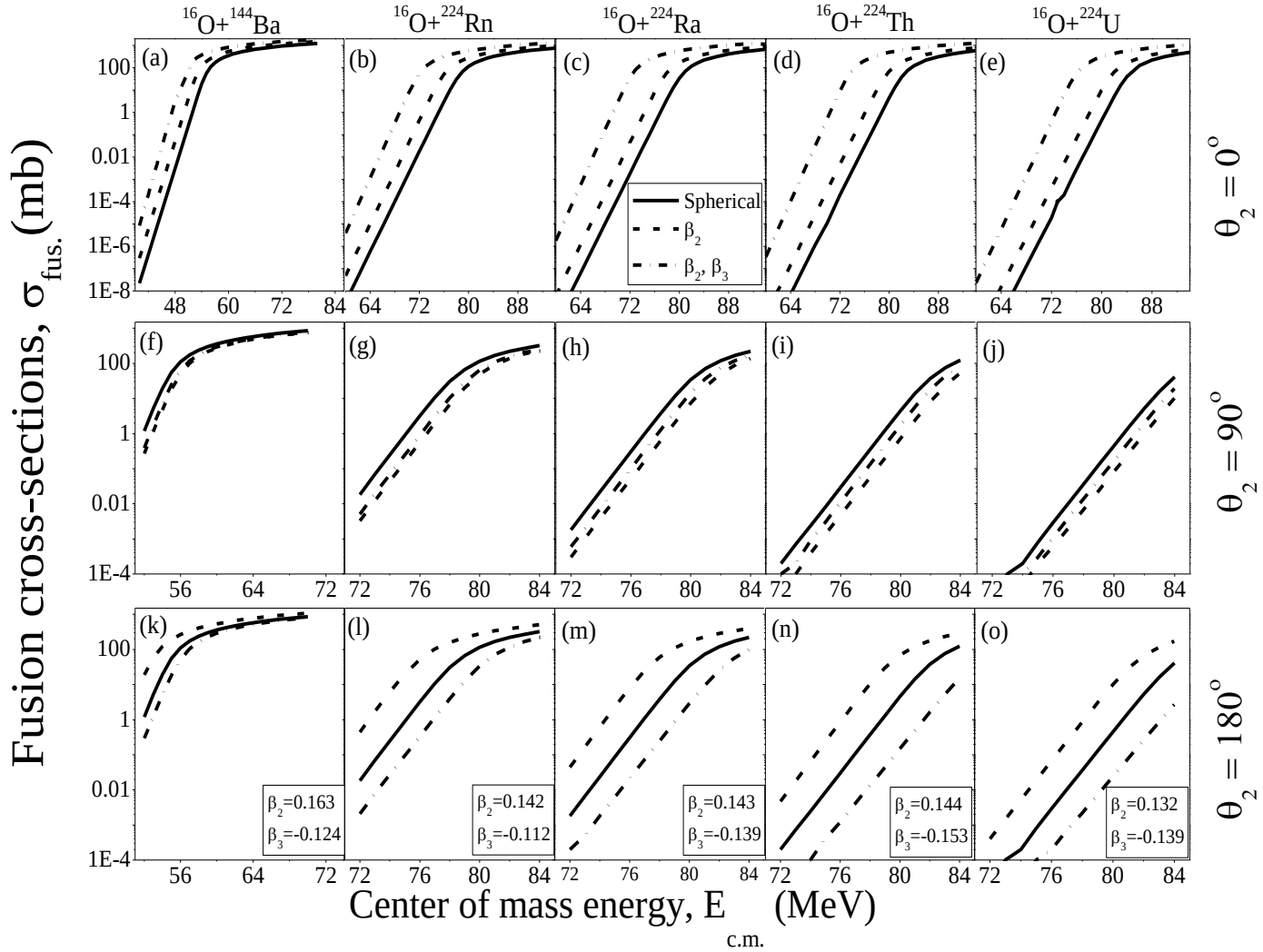

Figure 3.4 The fusion cross-sections ($\sigma_{fus.}$(mb)) as a function of center of mass energy ($E_{c.m.}$(MeV)) calculated using Wong formula upto octupole deformed choices of $^{16}O+^{144}Ba$, ^{224}Rn, ^{224}Ra, ^{224}Th, and ^{224}U reactions at different orientations ($\theta_2=0^o$, 90^o, and 180^o).

In Fig. 3.4, the fusion cross-sections calculated using Wong formula are depicted at different orientation upto octupole deformed choices of nuclei as mentioned above. From this it has been observed that the octupole deformed ($\beta_3 < 0$) nuclei gives largest amount of fusion cross-section σ_{fus}(mb) when there is no orientation, i.e. $\theta_2=0^o$. On the other hand, the spherical cases gives the lowest σ_{fus}(mb) . With the inclusion of orientation, there is very small difference in the magnitude of σ_{fus}(mb) at $\theta_2=90^o$ for spherical, quadrupole and octupole deformed cases. Furthermore, at $\theta_2=180^o$, the σ_{fus}(mb) obtained from spherical and quadrupole are exactly same as obtained at $\theta_2=0^o$. However, the fusion cross-sections for $\beta_3 < 0$ becomes lowest at $\theta_2=180^o$.

Consequently, it can be said that the influence of β_3 can be seen by taking integration over angles θ_2= 0° to 360°. Moreover, the values of fusion cross-sections obtained using Wong formula are listed in Table 3.2 for selected choices of octupole deformed nuclear systems.

Table 3.2 Fusion cross-sections calculated using Wong formula for different nuclear reactions at orientations, θ_2=0°, 90°, 180°.

$^{16}O+^{144}Ba\rightarrow^{160}Gd^*$

$E_{c.m.}$	T	Fusion cross-sections, σ_{fus}(mb)								
		θ_2=0°			θ_2=90°			θ_2=180°		
(MeV)	(MeV)	Sph.	Quad.	Oct.	Sph.	Quad.	Oct.	Sph.	Quad.	Oct.
52	0.215	1.20	18.97	209.51	1.20	0.27	0.39	1.20	18.97	0.30
53	0.217	5.10	57.51	295.58	5.10	1.15	1.67	5.10	57.51	1.24
54	0.220	470.05	120.64	379.34	470.05	4.77	6.88	470.05	120.64	5.02
55	0.222	55.10	193.16	460.23	55.10	17.73	24.45	55.10	193.16	18.23
56	0.224	19.29	266.27	538.26	19.29	50.28	63.57	19.29	266.27	51.71
57	0.226	110.62	337.52	613.65	110.62	101.21	118.43	110.62	337.52	104.91
58	0.228	173.23	406.48	686.35	173.23	159.15	177.79	173.23	406.48	166.19
59	0.230	236.12	473.12	756.59	236.12	217.58	236.79	236.12	473.12	228.38
60	0.232	297.45	537.56	824.49	297.45	274.66	294.22	297.45	537.56	289.16
61	0.234	356.86	599.88	890.16	356.86	329.99	349.87	356.86	599.88	348.11
62	0.235	414.41	660.26	953.71	414.41	383.63	403.71	414.41	660.26	405.19
63	0.237	523.93	718.66	1015.25	523.93	435.52	455.89	523.93	718.66	460.48
64	0.239	576.12	775.23	1074.86	576.12	485.78	506.41	576.12	775.23	514.03
65	0.241	626.70	830.06	1132.64	626.70	534.50	555.37	626.70	830.06	565.94
66	0.243	675.76	883.23	1188.67	675.76	581.74	602.84	675.76	883.23	616.40
67	0.245	723.34	934.81	1243.20	723.34	627.57	648.90	723.34	934.81	665.23
68	0.247	769.53	984.87	1295.96	769.53	672.06	693.91	769.53	984.87	712.64
69	0.248	814.51	1033.47	1347.19	814.51	715.25	737.14	814.51	1033.47	758.66
70	0.250	857.95	1080.85	1396.96	857.95	757.21	779.31	857.95	1080.85	803.38

$^{16}O+^{224}Rn\rightarrow^{240}Pu^*$

$E_{c.m.}$	T	Fusion cross-sections, σ_{fus}(mb)								
		θ_2=0°			θ_2=90°			θ_2=180°		
(MeV)	(MeV)	Sph.	Quad.	Oct.	Sph.	Quad.	Oct.	Sph.	Quad.	Oct.
72	0.154	0.02	0.44	56.94	0.02	0.00	0.01	0.02	0.44	0.00
73	0.155	0.07	1.68	115.97	0.07	0.01	0.02	0.07	1.68	0.01
74	0.157	0.25	6.12	184.58	0.25	0.04	0.07	0.25	6.12	0.03
75	0.158	0.90	20.02	254.77	0.90	0.16	0.25	0.90	20.02	0.09
76	0.160	3.19	52.27	323.98	3.19	0.56	0.89	3.19	52.27	0.33
77	0.162	10.66	102.41	391.60	10.66	1.97	3.13	10.66	102.41	1.15
78	0.163	30.52	160.78	457.53	30.52	6.70	10.37	30.52	160.78	3.93
79	0.165	67.27	220.80	521.84	67.27	20.25	29.30	67.27	220.80	12.51
80	0.166	115.27	280.20	584.52	115.27	48.82	64.03	115.27	280.20	33.77
81	0.168	167.03	338.35	645.65	167.03	90.49	109.32	167.03	338.35	70.92
82	0.169	219.04	395.14	705.28	219.04	137.89	158.19	219.04	395.14	118.14
83	0.171	270.22	450.58	763.48	270.22	186.43	207.33	270.22	450.58	168.69
84	0.172	320.30	504.71	820.30	320.30	234.48	255.72	320.30	504.71	219.44

$^{16}O+^{224}Ra \rightarrow ^{240}Cm^{*}$										
$E_{c.m.}$	T	Fusion cross-sections, σ_{fus} (mb)								
		$\theta_2=0^o$			$\theta_2=90^o$			$\theta_2=180^o$		
(MeV)	(MeV)	Sph.	Quad.	Oct.	Sph.	Quad.	Oct.	Sph.	Quad.	Oct.
72	0.144	0.00	0.04	36.89	0.00	0.00	0.00	0.00	0.04	0.00
73	0.146	0.01	0.17	87.87	0.01	0.00	0.00	0.01	0.17	0.00
74	0.147	0.02	0.61	155.16	0.02	0.00	0.01	0.02	0.61	0.00
75	0.149	0.08	2.26	227.10	0.08	0.01	0.03	0.08	2.26	0.01
76	0.151	0.31	7.95	298.76	0.31	0.05	0.10	0.31	7.95	0.02
77	0.152	1.09	24.74	368.95	1.09	0.18	0.36	1.09	24.74	0.07
78	0.154	3.81	60.32	437.44	3.81	0.64	1.28	3.81	60.32	0.25
79	0.156	12.42	111.61	504.22	12.42	2.22	4.47	12.42	111.61	0.85
80	0.157	34.04	169.23	569.33	34.04	7.39	14.32	34.04	169.23	2.86
81	0.159	71.77	227.86	632.83	71.77	21.77	37.74	71.77	227.86	9.10
82	0.160	119.35	285.73	694.79	119.35	50.92	76.00	119.35	285.73	25.51
83	0.162	170.02	342.36	755.25	170.02	92.25	122.22	170.02	342.36	57.02
84	0.164	220.78	397.70	814.28	220.78	138.68	170.68	220.78	397.70	100.28

$^{16}O+^{224}Th \rightarrow ^{240}Cf^{*}$										
$E_{c.m.}$	T	Fusion cross-sections, σ_{fus} (mb)								
		$\theta_2=0^o$			$\theta_2=90^o$			$\theta_2=180^o$		
(MeV)	(MeV)	Sph.	Quad.	Oct.	Sph.	Quad.	Oct.	Sph.	Quad.	Oct.
72	0.144	0.00	0.00	8.88	0.00	0.00	0.00	0.00	0.00	0.00
73	0.146	0.00	0.02	30.22	0.00	0.00	0.00	0.00	0.02	0.00
74	0.147	0.00	0.06	76.47	0.00	0.00	0.00	0.00	0.06	0.00
75	0.149	0.01	0.23	141.50	0.01	0.00	0.00	0.01	0.23	0.00
76	0.151	0.03	0.85	212.73	0.03	0.00	0..0111	0.03	0.85	0.00
77	0.152	0.11	3.04	284.29	0.11	0.02	0.04	0.11	3.04	0.00
78	0.154	0.38	10.33	354.55	0.38	0.06	0.14	0.38	10.33	0.01
79	0.156	1.31	30.30	423.15	1.31	0.21	0.50	1.31	30.30	0.04
80	0.157	4.49	68.85	490.07	4.49	0.73	1.75	4.49	68.85	0.15
81	0.159	14.27	120.77	555.35	14.27	2.51	5.94	14.27	120.77	0.49
82	0.160	37.53	177.48	619.03	37.53	8.18	18.11	37.53	177.48	1.63
83	0.162	76.00	234.72	681.30	76.00	23.43	44.55	76.00	234.72	5.21
84	0.164	123.07	289.75	741.97	123.07	53.47	80.31	123.07	289.75	15.38

$^{16}O+^{224}U \rightarrow ^{240}Fm^{*}$										
$E_{c.m.}$	T	Fusion cross-sections, σ_{fus} (mb)								
		$\theta_2=0^o$			$\theta_2=90^o$			$\theta_2=180^o$		
(MeV)	(MeV)	Sph.	Quad.	Oct.	Sph.	Quad.	Oct.	Sph.	Quad.	Oct.
72	0.144	0.00	0.00	0.39	0.00	0.00	0.00	0.00	0.00	0.00
73	0.146	0.00	0.00	1.52	0.00	0.00	0.00	0.00	0.00	0.00
74	0.147	0.00	0.01	5.87	0.00	0.00	0.00	0.00	0.01	0.00
75	0.149	0.00	0.02	20.56	0.00	0.00	0.00	0.00	0.02	0.00
76	0.151	0.00	0.07	56.34	0.00	0.00	0.00	0.00	0.07	0.00
77	0.152	0.01	0.24	113.23	0.01	0.00	0.00	0.01	0.24	0.00
78	0.154	0.04	0.86	179.58	0.04	0.01	0.01	0.04	0.86	0.00
79	0.156	0.13	3.03	247.68	0.13	0.02	0.05	0.13	3.03	0.01
80	0.157	0.45	10.09	314.96	0.45	0.08	0.17	0.45	10.09	0.02

81	0.159	1.56	29.18	380.80	1.56	0.29	0.59	1.56	29.18	0.08
82	0.160	5.25	65.94	445.09	5.25	0.98	2.02	5.25	65.94	0.26
83	0.162	16.16	115.70	507.85	16.16	3.31	6.69	16.16	115.70	0.85
84	0.164	40.87	170.33	569.11	40.87	10.49	19.75	40.87	170.33	2.75

3.2 Conclusion and Summary:

In this work, the role of octupole deformed nuclei with the inclusion of orientations has been analyzed on the interaction potential. The barrier characteristics, i.e. barrier- height V_B(MeV) and barrier position R_B(fm), calculated for $^{16}O+^{144}Ba$, ^{224}Rn, ^{224}Ra, ^{224}Th, and ^{224}U reactions and are found to break symmetry around 90^o. Further, the optimum configuration for this case of octupole deformed ($\beta_3 < 0$) nuclei is found nearby 90^o. In the calculation of fusion cross-sections using Wong formula [1], the largest amount of $\sigma_{fus}(\mathrm{mb})$ is obtained for the case of octupole deformed nucleus when there is no orientation.

In future, it is of interest to investigate the overall effect of all the orientation of octupole deformed nuclei. For this the fusion cross-sections are to be integrated over all orientations and the results obtained would call for experimental verification.

Also it is interesting to explore the optimum orientations in view of octupole deformation, in general, for other possible combinations of deformations (i.e. β_2 and β_3).

References:

[1] C. Y. Wong, Phys. Rev. Lett. **31**, 766 (1973).